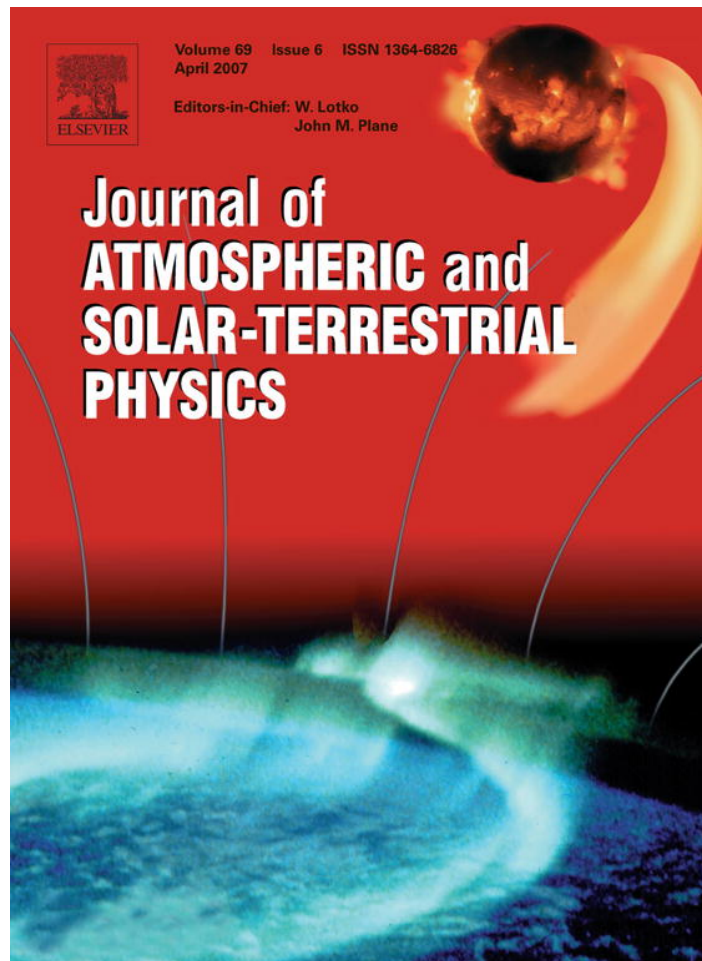


Provided for non-commercial research and educational use only.
Not for reproduction or distribution or commercial use.



This article was originally published in a journal published by Elsevier, and the attached copy is provided by Elsevier for the author's benefit and for the benefit of the author's institution, for non-commercial research and educational use including without limitation use in instruction at your institution, sending it to specific colleagues that you know, and providing a copy to your institution's administrator.

All other uses, reproduction and distribution, including without limitation commercial reprints, selling or licensing copies or access, or posting on open internet sites, your personal or institution's website or repository, are prohibited. For exceptions, permission may be sought for such use through Elsevier's permissions site at:

<http://www.elsevier.com/locate/permissionusematerial>



ELSEVIER

Journal of Atmospheric and Solar-Terrestrial Physics 69 (2007) 675–684

Journal of
ATMOSPHERIC AND
SOLAR-TERRESTRIAL
PHYSICS

www.elsevier.com/locate/jastp

Space storm as a phase transition

J.A. Wanliss^{a,*}, P. Dobias^b

^aERAU, 600 S. Clyde Morris Blvd, Daytona Beach, FL, USA

^bDRDC CORA, 101 Colonel By Dr., Ottawa, ON, Canada

Received 16 November 2005; received in revised form 15 November 2006; accepted 3 January 2007

Available online 14 January 2007

Abstract

Fluctuations of the *SYM-H* index were analyzed for several space storms preceded by more than a week of extremely quiet conditions to establish that there was a rapid and unidirectional change in the Hurst scaling exponent at the time of storm onset. That is, the transition was accompanied by the specific signature of a rapid unidirectional change in the temporal fractal scaling of fluctuations in *SYM-H*, signaling the formation of a new dynamical phase (or mode) which was considerably more organized than the background state. We compare these results to a model of multifractional Brownian motion and suggest that the relatively sudden change from a less correlated to a more correlated pattern of multiscale fluctuations at storm onset can be characterized in terms of nonequilibrium dynamical phase transitions. The results show that a dynamical transition in solar wind VB_s is correlated with the storm onset for intense storms, suggesting that the dynamical transition observed in *SYM-H* is of external solar wind origin, rather than internal magnetospheric origin. However, some results showed a dynamical transition in solar wind scaling exponents not matched by similar transitions in *SYM-H*. In other instances, we observed some small storms where there was a strong dynamical transition in *SYM-H* without similar changes in the VB_s scaling statistics, suggesting that changes were due to internal magnetospheric processes. In summary, the results for intense storms points to the solar wind as being responsible for providing the scale free properties in the *SYM-H* fluctuations but the evidence for small storms clearly limit the importance of the solar wind fluctuations; their interaction is more complex than simple causality.

© 2007 Elsevier Ltd. All rights reserved.

Keywords: Magnetosphere; Storms and substorms; Fractal modeling; Phase transitions

1. Introduction

Space storms include a variety of electromagnetic processes extending from the surface of the earth into the deep magnetosphere, with activity primarily near-earth. Recent studies on the causes of space storms have found that coronal mass ejections

(CMEs) and extreme values of the southward interplanetary magnetic fields appear to be key factors in storm development (Gonzalez et al., 1994; Richardson et al., 2001). Long-range interactions between the magnetosphere–ionosphere (MI) systems also play an important role in the initiation and development of space storms, and interaction between these two spheres is highly nonlinear (Lui, 2002; Daglis et al., 2003). The connection between solar wind fluctuations and storms is so strong that it is tempting to minimize the role of internal

*Corresponding author. Tel.: +1 386 2267750;
fax: +1 386 2266621.

E-mail address: wanlib01@erau.edu (J.A. Wanliss).

magnetospheric dynamics and to place virtually all the blame on the solar wind. That is why it is often thought that the problems of space weather can be solved in the main via accurate and more complete monitoring of the solar wind alone.

Here we present a study of certain statistical properties associated with space storms. We use these properties to investigate the nature of the transition of the magnetosphere from quiet times to times of intense space storms. While it is impossible to make definite conclusions from only a few events, we demonstrate that many storms can be characterized in context of a nonequilibrium system undergoing a dynamical phase transition. That is, the transition is accompanied by the specific signature of a rapid change in the temporal scaling of fluctuations in a storm-time geomagnetic index, signaling the formation of a new dynamical phase (or mode) which is considerably more organized than the background state. To facilitate our analysis, we characterized the behavior of the magnetosphere prior to, and during, space storms via the *SYM-H* index. *SYM-H* is a geomagnetic index which uses data from different ground-based magnetometer stations. The traditional index used in storm studies is *DST*, from which *SYM-H* differs by its cadence of one-minute rather than one hour, and slightly different convolution of the station data. These differences notwithstanding, the two indices are effectively interchangeable in an operational sense (Wanliss and Showalter, 2006).

Wanliss (2005) used a statistical physics approach to analyze fluctuations of *SYM-H* for the epoch 1981–2002 and separated quiet intervals from active intervals on the basis of the *Kp* index, a high-latitude index of magnetosphere activity. They found that active intervals had larger self-similarity scaling exponents than quiet intervals. In their study, however, all active intervals occurred during space storms. This may be important because it suggests that there is a common statistical behavior during quiet intervals different from the typical statistical behavior observed during active (storm) intervals. A trend towards higher scaling exponents was discovered for increasing magnetospheric activity, possibly implying an increase in organization with magnetospheric activity.

A change in scaling behavior of fluctuation statistics suggests symmetry-breaking and self-organized criticality (SOC). This may occur when a system is perturbed near a critical point (Chang, 1992; Chang et al., 2003, 2004). By critical we mean

that a single local perturbation can lead to effects that affect the whole system. Without discounting the possibility, it is nevertheless difficult to accept that the magnetosphere exists in a critical configuration during space storms, because as mentioned previously, these are generally understood to be a direct result of massive impulsive solar wind fluctuations impinging on the entire magnetopause with a more limited, though not necessarily unimportant, role assigned to internal magnetospheric dynamics. The classical view of storms seems to be *mostly correct* in that one can often link CMEs to subsequent storms (Huttunen et al., 2002). But some features cannot be explained by traditional models. While the development and gross morphology of space storms is fairly well understood, a consensus has not been reached regarding the trigger/s. CMEs and extreme values of southward IMF appear to be among the leading factors in storm development, although neither of these factors by themselves are sufficient nor necessary for occurrence or development. For example, during solar minimum different factors seem to drive storms (Webb et al., 2001). The solar wind is clearly the driver of storms, but the development and trigger mechanisms are cloudy.

The paper is organized as follows. In the following section we provide a brief outline of the methodology used to study large-scale correlations in the magnetosphere; we utilize detrended fluctuation analysis (DFA), which is similar to the structure function analysis, to analyze multiscale fractal properties of data. Section 3 contains results of our analysis on *SYM-H*. We also discuss the influence of the solar wind on the storm dynamics via analysis of many solar wind parameters, including the coupling function $V B_s$. Section 4 outlines the possibility of interpreting the results as a dynamical phase transition, and presents arguments in favor of such an interpretation. We consider the possibility that at least some storms can be modeled as a dynamical phase transition described by multifractional Brownian motion (mfBm). At the end we briefly summarize our findings.

2. Methods

A signal $B(t)$ that displays fractional Brownian motion (fBm) is one for which both the real and imaginary components of the Fourier amplitudes are Gaussian-distributed random variables (Hergar-

ten, 2002). As well, the mean of the Fourier amplitudes $\varphi(v) = 0$ and $\varphi(v)\varphi(v')^* = P(v)\delta(v - v')$, where $P(v) \sim |v|^{-2\alpha-1}$. This means that for $\alpha = \frac{1}{2}$, fBm reduces to the random walk with power law spectrum varying as an inverse square. Signals with scaling exponents above $\alpha = \frac{1}{2}$ are called persistent, because if the data at some point have $B(t_{i+1}) > B(t_i)$, for example, then the probability is greater than 0.5 that $B(t_{i+2}) > B(t_{i+1})$. Signals with exponents below $\frac{1}{2}$ are called antipersistent because if $B(t_{i+1}) > B(t_i)$, the probability is greater than 0.5 that $B(t_{i+2}) < B(t_{i+1})$. Typically, fBm is nonstationary, and detection of memory is a delicate task. Nonstationarity means that statistical properties are not constant through the signal, and traditional analysis methods that assume stationarity cannot be used. Fig. 1 shows examples of fBm calculated from the Wood–Chan circulant method (Wood and Chan, 1994). The roughness of the curves is greater for smaller values of the scaling exponent.

The multifractional Brownian motion (mfBm) is a generalized version of fBm in which the scaling exponent α is no longer a constant, but a function of the time index (Peltier and Levy Vehel, 1995). In this case the increments of mfBm are nonstationary and the process is no longer self-similar. Fig. 2 shows a simple example of a mfBm where the scaling exponent does not change continuously but as a step functional parameter; it has a value $\alpha = 0.5$ for

the first half of the series and $\alpha = 0.7$ for the rest. This is a special case of mfBm called a step fractional Brownian motion (Benassi et al., 2000). The abrupt transition is clear from Fig. 2a because the smoothness of the series changes suddenly. An abrupt change like this is characteristic of systems that undergo a phase transition or attain a new

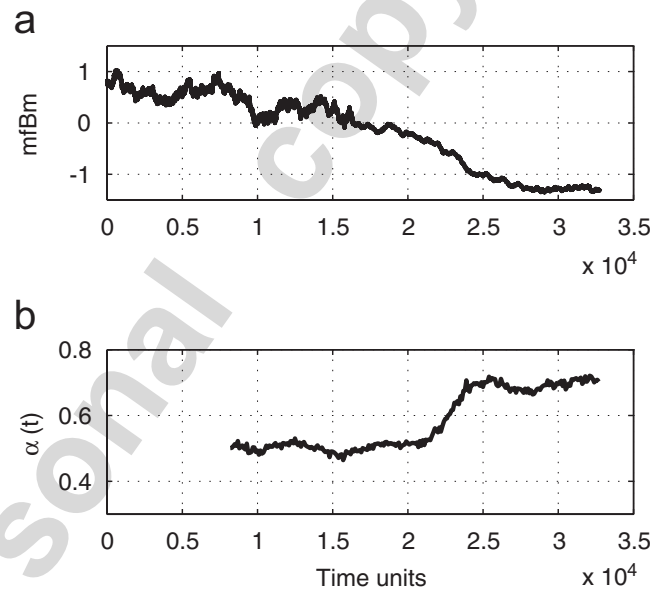


Fig. 2. (a) Model step mfBm calculated by splicing together two fBm series with $\alpha = 0.5$ and $\alpha = 0.7$. (b) Scaling exponent $\alpha(t)$ computed from DFA.

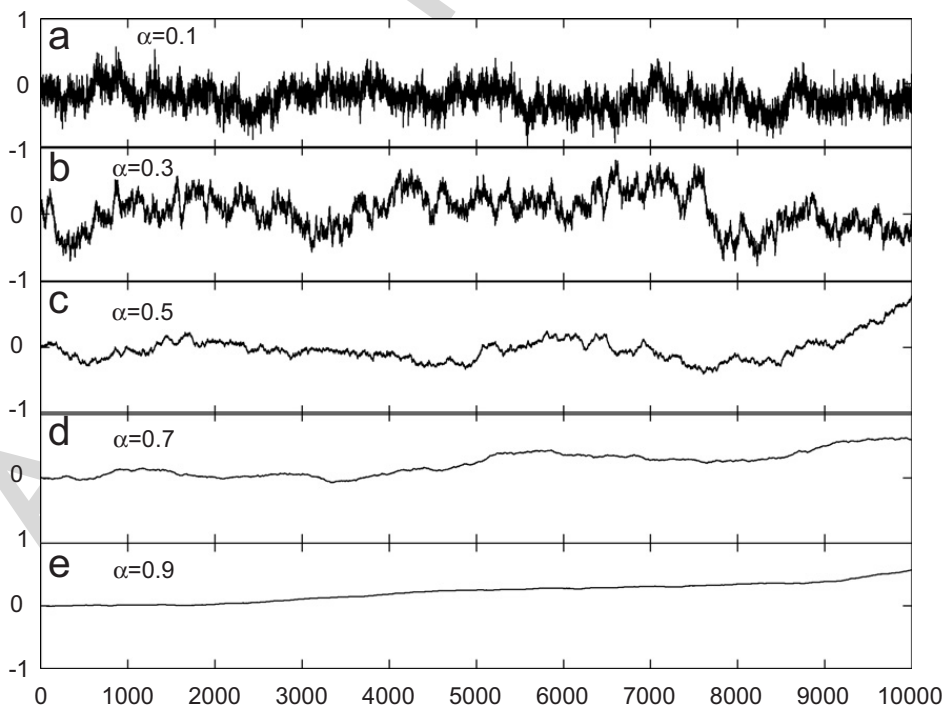


Fig. 1. Examples of fBm for different values of the scaling exponent.

dynamical phase or mode. For instance in an equilibrium system a phase transition in water (evaporation/condensation) brings about a change in long-range correlations in molecular motion. Obviously, the free Brownian motion of gas molecules is not reproducible in a fluid. In this case the motion of molecules is highly correlated due to strong intermolecular forces. Therefore, the phase transition is characterized by a change in scaling parameter that characterizes correlation of molecular motion. The magnetosphere, however, is a nonequilibrium system so such a change in the observed scaling exponent is certainly not evidence of a phase transition in the classical sense. Nonequilibrium systems showing strong evidence of SOC—the magnetosphere is a good example (Chang, 1992; Chang et al., 2003, 2004)—can be described in terms of absorbing-state phase transitions (Dickman et al., 1998; Dickman, 2002; Alava, 2003; Muñoz et al., 2001). In this case a change in scaling exponent suggests symmetry-breaking and SOC. In nonequilibrium systems such a change may be referred to as a *dynamical phase transition*.

To examine these simulated model data, shown in Fig. 2a, one can study how a fluctuation measure, denoted here by F , scales with the size n of the time window considered. Specific methods, such as Hurst's rescaled range analysis, power spectral analysis, structure function analysis, or DFA, all essentially calculate such a fluctuation measure. Typically, $F \propto n^\alpha$, where α is the scaling exponent; in the present example, the scaling exponent is also known as the Hurst exponent. Power laws like this are the signature of a propagation of information across the system. Several of the above methods have been used previously to analyze data relevant to space physics (e.g. Takalo et al., 1993; Consolini and De Michelis, 1998; Freeman et al., 2000; Wanliss and Reynolds, 2003; Wanliss, 2004, 2005; Wanliss et al., 2005; Uritsky et al., 2006).

In this paper we employ DFA (Peng et al., 1995). The method is a modified root mean squared analysis of a random walk designed specifically to deal with nonstationarities in nonlinear data. It is among the most robust of statistical techniques designed to detect long-range correlations. DFA is robust to the presence of trends (Hu et al., 2001) and nonstationary time series (Chen et al., 2002) and is thus a good choice for analysis of mfBm. In short, the technique begins by the division of the time series into boxes of different length, n . After

this, a least squares quadratic fit to the data signal is performed for each box which represents the local trend in each box. Next, for each box the root mean squared deviations, $F(n)$, of the signal from the local trend is determined. Different box sizes are selected and the procedure is repeated. Finally, if the fluctuation is a power law, the scaling exponent is computed from the slope of the log–log plot of deviation versus box size.

Rather than simply probe the existence of correlated behavior over the entire *SYM-H* time series, what we do is find a “local measurement” of the degree of long-range correlations described by the variations of the scaling exponent during a space storm. The probe used is the observation box of length 8192 min (5.7 days); this box is placed at the beginning of the data, and then the scaling exponent $\alpha(t_i)$ is calculated for the data contained in the box. Time t_i is the universal time of the last point in the box. The first value for $\alpha(t_i)$ occurs at $i = 8192$. Next, the box is shifted right one point along the series, and the scaling exponent for the new box is calculated. This procedure is iterated for the entire sequence; for the storm this will encompass the quiet preceding the storm through the end of the recovery phase, and beyond. This procedure was followed to calculate Fig. 2b which shows the variation of the calculated scaling exponent, $\alpha(t)$. One can see from this figure that the DFA technique accurately recovers the scaling exponent of a simple step mfBm. Note however that although the step mfBm model features a *discontinuous* jump in the scaling exponent, the time dependent DFA numerical technique does not immediately capture the change, but takes some time to transition in a unidirectional fashion from the smaller to larger exponent.

3. Analysis and results

3.1. *SYM-H* multiscaling

We examined the *SYM-H* dataset for 1999 and 2000 and considered only events where a space storm with $SYM-H < -100$ nT was preceded by at least seven days of relative quiescence, with typical values of $SYM-H > -50$ nT. The events selected were thus isolated in nature and featured only small changes in *SYM-H* and little notable dynamic activity prior to storm onset. We selected events on this basis because of earlier evidence that quiet intervals have statistically different properties from

active intervals. By considering storms preceded by long quiet intervals we expected to capture the quiet time scaling exponent with values near $\alpha \sim 0.52 \pm 0.04$ (Wanliss, 2005), and then potentially a transition to larger values as the active storm begins. The intervals we examined began at times T_0 on January 1, 1999 at 11 UT, February 3, 1999 at 19 UT, and January 13, 2000 at 3 UT, June 29, 2000 at 16 UT; the *SYM-H* data are show in Figs. 3a,b,e,f. Dashed-dot lines indicate the moderate and intense storm boundaries at -50 and -100 nT. We now present

results from DFA analysis of these four storms as observed via changes in *SYM-H*.

The solid line in Figs. 3c,d,g,h show the respective time dependent *SYM-H* scaling exponent for each event. Horizontal dashed-dot lines indicate the $\alpha(t) \sim 0.5$ Brownian motion value and the approximate time of the space storm main phase (vertical line). For the event of January 1, 1999 the scaling exponent ranges approximately between values of 0.6 and 0.5 before the start of the storm with a decreasing trend noticeable early on in the data.

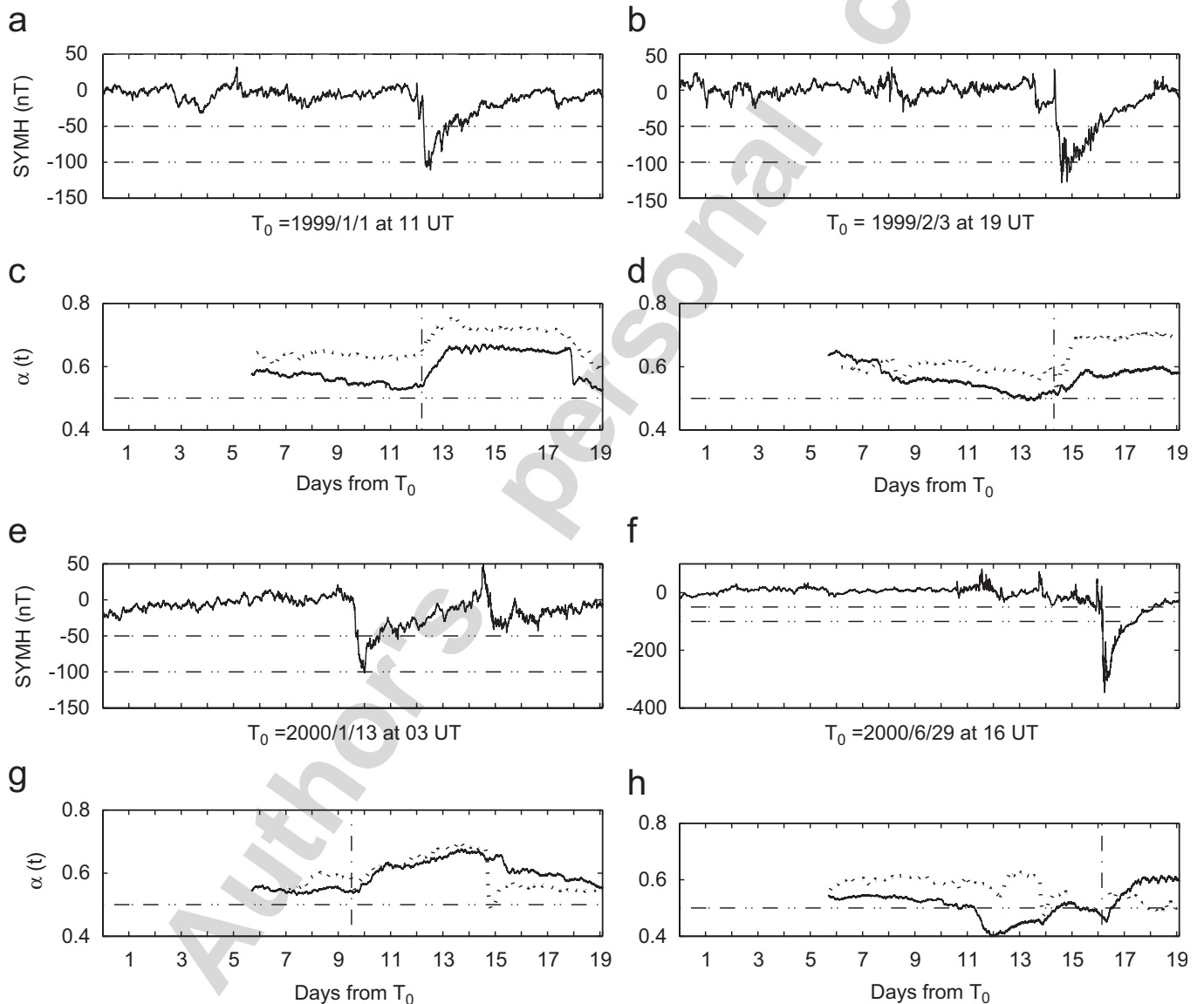


Fig. 3. Solid lines show *SYM-H* and associated time dependent scaling exponents $\alpha(t)$ for the events of (a,c) January 1, 1999 from 11 UT; (b,d) April 4, 1999 at 19 UT; (e,g), January 13, 2000 at 3 UT; and (f,h) June 29, 2000 at 16 UT. Horizontal dashed-dot lines in the *SYM-H* plots indicate the moderate and intense storm boundaries at -50 and -100 nT. Ticks on the abscissa equal one day intervals. Horizontal dashed-dot lines in the scaling exponent plots indicate the $\alpha(t) \sim 0.5$ Brownian motion value and the approximate time of the space storm main phase is indicated by the vertical line. The dotted curves represent $\alpha(t)$ for the associated solar wind VB_s , which was ballistically propagated to the earth.

Near the approach of storm onset the scaling exponent settles down and fluctuates near a value of 0.5, suggestive of Brownian motion. Around the time of onset the exponent rapidly jumps to ~ 0.7 and stays approximately constant for several days. The rapid jump is an indication of a transition from a highly random state or mode to one that is more ordered and predictable; the shape of the curve for $\alpha(t)$ is strongly reminiscent of the DFA results for the step mfBm model data in Fig. 2b which features a discontinuous jump in the scaling exponent. Even though the energetics of the main and recovery phases are quite different the scaling exponent remains constant after the main phase indicating that the magnetospheric response to reduced solar wind energy input is statistically similar. It was only after *SYM-H* returned to pre-storm values, near 0 nT, that the inner magnetosphere appears to undergo another sharp transition in scaling exponent. Five days after storm onset the scaling exponent attained values akin to the pre-storm situation.

The other three events feature the same general behavior, although none resemble the step mfBm model as clearly as the January 1999 event; each case features smaller scaling exponent hovering near 0.5 preceding the storm onset and a jump to a larger value once the storm has begun. The event of February 3, 1999 is interesting in that the start of the jump in exponent occurred a day before the storm began, around the middle of day 13 after T_0 (Fig. 3d). This occurred when *SYM-H* (Fig. 3b) dropped rapidly before recovering and entering the initial phase of the storm proper. The event of June 29, 2000 is also interesting in that the scaling exponent exhibited considerable variability prior to the storm onset, dropping as low as $\alpha \approx 0.4$ around day 12 after T_0 (Fig. 3h). This antipersistent value of scaling exponent matched very well with the sudden increase and change in roughness of *SYM-H* (Fig. 3f). Although this storm had a massive *SYM-H* perturbation (minimum -347 nT) the time from immediately before the start of the storm featured scaling exponent behavior that was very similar to both the January 1999 event, and the step mfBm dynamical phase transition model.

3.2. Solar wind control and multiscaling

The value of the *SYM-H* scaling exponent before the intense space storm was close to the Brownian value ($\alpha = 0.5$) suggesting the pre-storm magneto-

spheric statistical state was highly disordered. This continued until the statistical state of the nonequilibrium system passed into the more ordered and imitative state of the space storm main phase. There are at least two possible sources for this change. One possibility is that the process causing the change in scale-free properties was strongly dominated by the dynamics internal to the magnetosphere, and scaling behavior of the measured exponents is intrinsic.

The other possibility is that the change in scaling exponent is in some sense a reflection of the scale-free properties of the solar wind to which the magnetosphere is so strongly coupled (e.g. Freeman et al., 2000). For some time now the turbulent nature of the solar wind has been well known (Burlaga et al., 1989; Burlaga, 1991). Other studies have indicated the existence of turbulence in the plasma sheet as well (Borovsky et al., 1997; Weygand et al., 2005), and the scaling behavior of the distribution functions in the plasma sheet are similar to that found for the solar wind. Thus it is possible that the dynamical transition observed in magnetospheric *SYM-H* scaling statistics could be a manifestation of a similar transition in the solar wind. To gain some insight into the latter option, we analyzed the solar wind parameters (in GSM coordinates) around the time of the events studied. Data were propagated to the dayside magnetopause using the Weimer et al. (2003) method and interpolated with 1 min cadence.

The events with the change in *SYM-H* scaling exponent most consistent with the step mfBm model are for January 1999 and June 2000. Consider the January 1999 event; near storm onset the density was 20 cm^{-3} and the solar wind speed just over 400 km/s. Data from ACE (not shown) indicate a jump in proton density and in solar wind velocity that were closely associated in time with the storm onset. The sudden drop of *SYM-H* to below -100 nT, was correlated with a large drop in the B_z component, from about $+10$ to -15 nT. For almost 7 h after this drop the values of B_z and the total magnetic field remained nearly constant. When B_z suddenly jumped back to $+10$ nT this signaled the start of the recovery phase and steady increase to pre-storm *SYM-H* values. The switch back to positive values of B_z did not influence the *SYM-H* correlation statistics, which remained close to $\alpha \sim 0.7$ (Fig. 3c, solid line), so B_z was not a simple control parameter. It is possible that a change in the B_z component contributed to the triggering of the

storm, but it was likely not the only cause. Observation of other solar wind variables, and combinations of variables, revealed no consistent pattern, although the strength of the interplanetary electric field appeared to be important for all of the events. Gaps in the June 2000 solar wind coverage do not allow correlations to be made.

As in Section 3.1 we also analyzed the temporal scaling properties of solar wind V , B , B_z , T , n , ε , and VB_s , which are, respectively, total speed, total interplanetary magnetic field, north–south component of the magnetic field, temperature, number density, solar wind power input function, and solar wind driving function where B_s is the rectified function of the north–south component of the interplanetary magnetic field. The parameters considered most likely to influence the magnetosphere are ε and VB_s , since they are known to be directly related to a component of the *AE* index (Tsurutani et al., 1990; Freeman et al., 2000; Uritsky et al., 2001; Watkins, 2002). The dotted curves in the plots of Fig. 3 show the associated $\alpha(t)$ for VB_s with 0.4 added to aid comparison with the associated *SYM-H* scaling exponent.

For all events the solar wind parameters mentioned above had scaling exponents $\alpha(t) < 0.5$ with average values near 0.33, consistent with the Kolmogorov (1941) model for inertial range turbulence in an incompressible fluid. This observation has been demonstrated many times before (e.g. Burlaga and Klein, 1986; Burlaga, 1991, 1993; Tu and Marsch, 1995; Hnat et al., 2002).

The event of January 1999 (Figs. 3a,c) had *SYM-H* and VB_s scaling exponent $\alpha(t)$ curves with similar shape. The scaling exponent curve for ε (not shown) showed no jump at storm onset and stayed nearly constant for the entire interval. At onset of the intense space storm the event of February 1999 also showed a clear jump in VB_s , but not in ε . The event of January 2000 showed no clear jump in VB_s , but ε does show a clear jump. Although tempting it would be incorrect to conclude that the similar shapes of the *SYM-H* and VB_s scaling exponent curves $\alpha(t)$ implies that the jump in the scaling exponent for *SYM-H* was caused by the $\alpha(t)$ jump observed in VB_s for the first two events. It has been demonstrated previously that it can be problematic to attempt direct comparisons of the fractal scaling exponents from geomagnetic indices and the solar wind (Chang and Consolini, 2001; Watkins, 2002), due to the possible multifractal scaling of the solar wind variables (Burlaga, 1991, 1992, 1993; Watkins

et al., 2006). The similarity in the shape of the *SYM-H* and VB_s scaling exponents is nevertheless an important signal because it suggests some coupling of the nonlinear statistical features of the solar wind and magnetospheric time series.

To compare the *SYM-H* and VB_s scaling exponents we first calculated the cross correlation function and the correlation coefficient. In all cases the cross correlation function showed a strong peak at a lag of zero minutes. For the January 1999 event the correlation coefficient between the sets of scaling exponents was $r = 0.943$, indicating a very strong correlation even though the correlation of the raw variables was low. Finally, the computed probability density functions of the derivative ($d\alpha(t)/dt$) were both well-fit by normal distributions; i.e. except for their baseline values, the shape and distributions of the scaling exponent values were similar. For the February 1999 event the correlation coefficient for the whole event is $r = 0.525$, but when it was calculated from day 11 (just over 3 days before storm onset) we found a significant correlation of $r = 0.961$. For the January 2000 event $r = 0.596$, but the correlation was again much more significant ($r = 0.964$) if the comparison was made only with data prior to day 14. These results indicate that while scaling exponent development of *SYM-H* and VB_s can be quite different in shape before the storm or long after it (with low correlation coefficient), the correlation became much better through the interval immediately preceding and following the intense space storm.

Scaling exponents for the other solar wind variables sometimes also displayed strong correlation with the *SYM-H* exponent, but we were not able to discern a consistent pattern. For example, for the January 1999 event (Figs. 3a,c) the *SYM-H* scaling exponent featured a sharp drop near day 18, possibly associated with the small space storm (*SYM-H* < -30 nT) observed just prior to the drop in scaling exponent. There were no equivalent changes in the VB_s scaling exponent. Neither did the raw solar wind data reveal clear signals except in the number density that doubles to about 20 cm^{-3} at this time. The VB_s scaling exponent for the event of January 2000 increased steadily but did not exhibit a strong jump at the time of storm onset; the exponent for the ε parameter exhibited a strong unidirectional jump. Furthermore, around the middle of day 14 there was a sharp drop in the value of the VB_s scaling exponent at the same time as the onset of a small space storm (Figs. 3e,g). This small

storm was clearly associated with a strong rotation of the IMF (with large southward B_z) and a ramp in the density (from about 10 to 120 cm⁻³) and V_x (from about 400 to 800 km/s). In this case there was a dynamical transition in the VB_s scaling exponent but no similar transition for the $SYM-H$ exponent. There is clearly not a one-to-one correspondence between the scaling statistics for $SYM-H$ and the solar wind, even for the strongly coupled VB_s function.

4. Discussion and summary

The analysis and results presented above show an interesting parallel between space storms and dynamical phase transitions. We analyzed four intense storms in terms of fluctuations in $SYM-H$ and detected scaling behavior that indicated a strong unidirectional transition from uncorrelated to correlated statistics around the start of the main phase. On average this transition was indicated by the change from $\alpha \sim 0.5$ prior to the storm onset and $\alpha > 0.6$ for some time after the onset. Such behavior has been observed in a range of stochastic systems and collections of data ranging from seismology to stock markets. It has been interpreted as a possibility of a phase transition in such nonequilibrium systems (Sornette, 2004).

The clear presence of fractal scaling behavior at all times and the difference in scaling exponents from quiet and active intervals suggests that the inner magnetosphere, with fluctuations represented by $SYM-H$, exists in a critical configuration. Whereas prior to the onset of the storm the nonlinear scaling exponent typically varied only slowly and continuously, storm onset resulted in a dramatic change such as might result from a dynamical phase transition. Transition to a lower energy state, such as for an intense space storm, results in more organization (larger scaling exponent). Once the excess energy has been dissipated during the recovery phase it results in less systemic organization and corresponding reduction in the scaling exponent to pre-storm values. This has possible operational value since the notion of a critical point has as one of its properties the ability to provide some universal predictions, even in the absence of a detailed model, by using what amounts essentially to generalized symmetry arguments.

The results of this study are rather promising and suggest that some storms can be described as dynamical phase transitions. For the events ana-

lyzed, all the necessary pieces seem to fall into place. We have not established whether the observed dynamical phase transitions are of internal magnetospheric origin, or whether they are caused by dynamical transitions in the solar wind driver. The results for intense storms point to the solar wind as being responsible for providing the scale-free properties in the $SYM-H$ fluctuations but the evidence for smaller storms clearly limit the importance of the solar wind fluctuations; the solar wind–magnetosphere interaction is more complex than simple causality.

In summary, we have studied the scaling properties of $SYM-H$ and solar wind variables during intervals containing intense (and smaller) space storms. It is clear that in some cases it is plausible that the transition in the $SYM-H$ scaling exponent could well be caused by a multiscale reorganization in the solar wind dynamics (e.g. the events from 1999). However, evidence of dynamical transitions in solar wind scaling exponents that do not match those observed in $SYM-H$ (January 2000 event at day 14.5, and June 2000 event at day 12) indicated that causality is not limited to the solar wind alone. For the January 1999 event there was a strong dynamical transition in $SYM-H$ associated with a small space storm without similar changes in the VB_s scaling statistics. This suggested to us the possibility of a coupling between the order and control parameters; i.e. internal magnetospheric dynamics, and that interaction with the solar wind driver, can play an important role in storm initiation and development, at least for small space storms. For intense space storms the results place the most important role on the solar wind driver, particularly VB_s .

The strong correlation in the development of the $SYM-H$ and VB_s scaling exponents during some intense space storms is important but should be interpreted with caution. By its essence $SYM-H$ is a time integrated signal, and VB_s is better described as a time series of increments (in terms of the fBm terminology). To properly compare the dynamics of scaling exponents of these signals, one should first construct a multiscale “filter” that would treat VB_s as input and $SYM-H$ as output. The extent to which this description is accurate will be shown through an investigation of a large suite of storms with variable magnitude and solar wind driving. One way to achieve this aim can be through the use of models based on stochastic fractional differential equations driven by Lévy noise. Equations in the general form

of stochastic fractional differential equations, for example,

$$(A_n \mathcal{D}^{\beta_n} + \dots + A_1 \mathcal{D}^{\beta_1} + A_0 \mathcal{D}^{\beta_0})B(t) = L(t)$$

are good model candidates because their asymptotic solutions display long-range dependence and second-order intermittency.

In the above equation $\beta_n > \beta_{n-1} > \dots > \beta_1 > \beta_0, n \geq 1, A_i \geq 0, i = 0, \dots, n$, and $L(t)$ is Lévy noise. \mathcal{D}^{β} is the Riemann–Liouville fractional derivative defined as

$$\mathcal{D}^{\beta} f(t) = \frac{1}{\Gamma(n-\beta)} \frac{d^n}{dt^n} \int_0^t (t-\tau)^{n-\beta-1} f(\tau) d\tau, \\ \beta \in [n-1, n), n = 1, 2, \dots$$

In conjunction with the multifractal behavior of the Lévy motion driving it, these equations would therefore be suitable to model time series with long-range dependence, second-order intermittency and multiscaling behavior, all of which appear to be important features of space physics observations.

Acknowledgments

This material is based upon work supported by the National Science Foundation under Grants No. 0449403 and 0417690. *SYM-H* data are from WDC-Kyoto. Solar wind data are from CDAWEB. We wish to thank Vadim Uritsky for his useful and detailed advice on the manuscript. SDG.

References

- Alava, M., 2003. Self-organized criticality as a phase transition. Eprint arXiv:cond-mat/0307688.
- Benassi, A., Bertrand, P., Cohen, S., Istaş, T., 2000. Identification of the Hurst index of a step fractional Brownian motion. *Statistical Inference Stochastic Processes* 3.
- Borovsky, J.R., Elphic, R.C., Funsten, H.O., Thomsen, M.F., 1997. The earth's plasma sheet as a laboratory for flow turbulence in high-beta MHD. *Journal of Plasma Physics* 57, 1–34.
- Burlaga, L.F., Klein, L.W., 1986. Fractal structure of the interplanetary magnetic field. *Journal of Geophysical Research* 91, 347–350.
- Burlaga, L.F., 1991. Multifractal structure of the interplanetary magnetic field near 25 AU: Voyager 2 observations near 25 AU 1987–1988. *Journal of Geophysical Research* 18, 69–72.
- Burlaga, L.F., 1992. Multifractal structure of the magnetic field and plasma in recurrent streams at 1-AU. *Journal of Geophysical Research* 97 (A4), 4283–4293.
- Burlaga, L.F., 1993. Intermittent turbulence in large-scale velocity fluctuations at 1 AU near solar maximum. *Journal of Geophysical Research* 98, 17467–17473.
- Burlaga, L.F., Mish, W.H., Roberts, D.A., 1989. Large-scale fluctuations in the solar wind at 1 AU: 1978–1982. *Journal of Geophysical Research* 94, 177–184.
- Chang, T., 1992. Low dimensional behavior and symmetry breaking of stochastic systems near criticality: can these effects be observed in space and in the laboratory? *IEEE Transactions on Plasma Science* 20, 691.
- Chang, T., Consolini, G., 2001. Magnetic field topology and criticality in geotail dynamics: relevance to substorm phenomena. *Space Science Reviews* 95 (1–2), 309–321.
- Chang, T.S., et al., 2003. Complexity, forced and/or self-organized criticality, and topological phase transitions in space plasmas. *Space Science Reviews* 107, 425–445.
- Chang, T., Tam, S.W.Y., Wu, C.C., 2004. Complexity induced anisotropic bimodal intermittent turbulence in space plasmas. *Physics of Plasmas* 11, 1287.
- Chen, Z., et al., 2002. Effect of nonstationarities on detrended fluctuation analysis. *Physical Review E* 65, 041107.
- Consolini, G., De Michelis, P., 1998. Non-Gaussian distribution function of *AE*-index fluctuations: evidence for time intermittency. *Geophysical Research Letters* 25, 4087–4090.
- Daglis, I.A., et al., 2003. Intense space storms: critical issues and open disputes. *Journal of Geophysical Research* 108 (A5), 1208.
- Dickman, R., 2002. Nonequilibrium phase transitions in epidemics and sandpiles. *Physica A* 306, doi:10.1016/S0378-4371(02)00488-0, 90–97.
- Dickman, R., Vespignani, A., Zapperi, S., 1998. Self-organized criticality as an absorbing-state phase transition. *Physical Review E* 57 (5), 5095–5105.
- Freeman, M.P., Watkins, N.W., Riley, D.J., 2000. Evidence for a solar wind origin of the power law burst lifetime distribution of the *AE* indices. *Geophysical Research Letters* 27, 1087–1090.
- Gonzalez, W.D., et al., 1994. What is a geomagnetic storm? *Journal of Geophysical Research* 99, 5771.
- Hergarten, S., 2002. *Self-organized Criticality in Earth Systems*. Springer Academic Press, Berlin, New York, p. 49.
- Hnat, B., Chapman, S.C., Rowlands, G., Watkins, N.W., Freeman, M.P., 2002. Scaling of solar wind ϵ and the *AU*, *AL*, and *AE* indices as seen by WIND. *Geophysical Research Letters* 29 (22), 2078.
- Hu, K., et al., 2001. Effect of trends on detrended fluctuation analysis. *Physical Review E* 64, 011114.
- Huttunen, K.E.J., et al., 2002. April 2000 magnetic storm: solar wind driver and magnetospheric response. *Journal of Geophysical Research* 107 (A12), 1440.
- Kolmogorov, A.N., 1941. Local structure of turbulence in incompressible fluid. *Doklady Akademii Nauk SSSR* 30, 299.
- Muñoz, M.A., Dickman, R., Pastor-Satorras, R., Vespignani, A., Zapperi S., 2001. Sandpiles and absorbing-state phase transitions: recent results and open problems. In: Marro, J., Garrido, P.L. (Eds.), *Modeling Complex Systems*. AIP Conference Proceedings, vol. 574, p. 102.
- Peltier, R., Levy Vehel, J., 1995. Multifractal Brownian motion: definition and preliminary results. Technical Report INRIA 2645.
- Peng, C.-K., et al., 1995. Quantification of scaling exponents and crossover phenomena in nonstationary heartbeat timeseries. *Chaos* 5 (1), 82–87.
- Richardson, I.G., Cliver, E.W., Cane, H.V., 2001. Sources of geomagnetic storms for solar minimum and maximum conditions during 1972–2000. *Geophysical Research Letters* 28, 2569–2572.

- Sornette, D., 2004. Critical Phenomena in Natural Sciences. Springer, Berlin.
- Takalo, J., Timonen, J., Koskinen, H., 1993. Correlation dimension and affinity of *AE* data and bicolored noise. *Geophysical Research Letters* 20, 1527–1530.
- Tsurutani, B.T., Sugiura, M., Iyemori, M., et al., 1990. The nonlinear response of *AE* to the IMF *B_y* driver—a spectral break at 5 hours. *Geophysical Research Letters* 17 (3), 279–282.
- Tu, C.-Y., Marsch, E., 1995. MHD structures, waves and turbulence in the solar wind: observations and theories. *Space Science Review* 73, 1–210.
- Uritsky, V.M., Klimas, A.J., Vassiliadis, D., 2001. Comparative study of dynamical critical scaling in the auroral electrojet index versus solar wind fluctuations. *Geophysical Research Letters* 28, 3809–3812.
- Uritsky, V.M., Klimas, A.J., Vassiliadis, D., 2006. Analysis and prediction of high-latitude geomagnetic disturbances based on a self-organized criticality framework. *Advances Space in Research* 37, 539–546.
- Wanliss, J.A., 2004. Nonlinear variability of *SYM-H* over two solar cycles. *Earth Planets Space* 56, e13–e16.
- Wanliss, J.A., 2005. Fractal properties of *SYM-H* during quiet and active times. *Journal of Geophysical Research* 110, A03202.
- Wanliss, J.A., Reynolds, M.A., 2003. Fractal dimension of low-latitude geomagnetic temporal variations. *Annales de Geophysicae* 21, 2025–2030.
- Wanliss, J.A., Showalter, K., 2006. The high resolution global storm index: DST versus *SYM-H*. *Journal of Geophysical Research* 111, A02202.
- Wanliss, J.A., et al., 2005. Multifractal modeling of magnetic storms via symbolic dynamics analysis. *Journal of Geophysical Research*, doi:10.1029/2004JA010996.
- Watkins, N.W., 2002. Scaling in the space climatology of the auroral indices: is SOC the only possible explanation? *Nonlinear Processes in Geophysics* 9 (5–6), 389–397.
- Watkins, N.W., Credington, D., Hnat, B., Chapman, S.C., Freeman, M.P., Greenhough, J., 2006. Toward synthesis of solar wind and geomagnetic scaling exponents: a fractional Levy motion model, in review.
- Webb, D.F., et al., 2001. The solar sources of geoeffective structures. In: Song, P., et al., (Ed.), *Space Weather*, AGU Geophysical Monograph 125, pp. 123–141.
- Weimer, D.R., Ober, D.M., Maynard, N.C., Collier, M.R., McComas, D.J., Ness, N.F., Smith, C.W., Watermann, J., 2003. Predicting interplanetary magnetic field (IMF) propagation delay times using the minimum variance technique. *Journal of Geophysical Research* 108(A1), doi:10.1029/2002JA009405, 1026.
- Weygand, J.M., et al., 2005. Plasma sheet turbulence observed by Cluster II. *Journal of Geophysical Research* 110, A01205.
- Wood, A., Chan, G., 1994. Simulation of Stationary Gaussian Processes. *Journal of Computational and Graphical Statistics* 3, 409–432.